Estimate of 2011 Abundance of the Bering-Chukchi-Beaufort Seas Bowhead Whale Population

G. H. Givens[*], S. L. Edmondson[*], J. C. George[†], R. Suydam[†],
R.A. Charif[‡], A. Rahaman[‡], D. Hawthorne[‡],
B. Tudor[†], R.A. DeLong[§] and C.W. Clark[‡]

May 17, 2013

Abstract

We estimate the total abundance of the Bering-Chukchi-Beaufort Seas population of bowhead whales (*Balaena mysticetus*) in 2011 from large datasets of visual sightings and acoustic locations. A Horvitz-Thompson type estimator is used, based on the numbers of whales counted at ice-based visual observation stations. It divides sightings counts by three correction factors. The first adjusts for detectability using the results of Givens et al. (2012), who estimate detection probabilities and their dependence on offshore distance, lead condition, and whale group size. The second correction adjusts for availability using the acoustic location data to estimate a time-varying smooth function of the probability that animals pass within visual range of the observation stations. The third correction accounts for missed visual watch effort. The mean correction factors are estimated to be 0.501 (detection), 0.619 (availability) and 0.520 (effort). The resulting 2011 abundance estimate is 16,892 with a 95% confidence interval of (15,704, 18,928). We also insert this estimate into a time series of past visual abundance estimates to estimate the rate of increase of the population. The annual increase rate is estimated to be 3.7% with a 95% confidence interval of (2.8%, 4.7%). These abundance and trend estimates are consistent with previous findings and are indicative of very low conservation risk for this population under the current indigenous whaling management scheme.

1 Introduction

In the spring of 2011, a major multi-faceted program of research for the Bering-Chukchi-Beaufort Seas population of bowhead whales (*Balaena mysticetus*) was undertaken, including ice-based visual counting, underwater acoustic monitoring, aerial photo-identification, satellite tagging and biopsy sampling. In this paper, we use the visual and acoustic data to estimate total bowhead population abundance and update the estimate of population increase rate.

[*]Department of Statistics, 1877 Campus Delivery, Colorado State University, Fort Collins, CO 80523 U.S.A. geof@lamar.colostate.edu. This work was supported by the North Slope Borough (Alaska) and the National Oceanic and Atmospheric Administration (through the Alaska Eskimo Whaling Commission).

[†]North Slope Borough, Department of Wildlife Management, Barrow AK, U.S.A.

[‡]Bioacoustics Research Program, Cornell Laboratory of Ornithology, Cornell University, Ithaca, NY 14850 U.S.A.

[§]DeLongView Enterprises, Box 85044, Fairbanks, AK 99708, U.S.A.

Our presentation is organized as follows. In the next section, we describe the available data. Detailed exposition of the survey protocols and available datasets are given by George et al. (2013) and Clark et al. (2013). Our statistical methods are explained in Section 3. Some portions of our approach rely on estimators whose statistical properties are derived in a technical appendix to avoid interrupting the flow of the paper. Analysis results follow in Section 4. The final section of the paper provides discussion and context for our findings.

2 Datasets

Our analyses use two datasets collected in the spring of 2011. The visual dataset was collected by ice-based observers sighting whales as they migrated to the northeast past Barrow, Alaska. Observers saw 3379 'New' and 632 'Conditional' whales from the primary observation perch[1]. The acoustic dataset was derived from continuous sound recordings from an array of 4 (initially) to 6 (later) passive underwater recorders placed on the seafloor in the vicinity of the visual observation perches and recovered later that summer. From these recordings, a subsample of time periods were examined to estimate whale locations from their calls and song. A total of 22,426 bowhead vocalizations yielding location estimates were collected.

The 2011 visual and acoustic data collection season ran from April 4, when the first visual watch was conducted on the ice edge, until July 27 when 6-channel acoustic recording ended. The first bowhead whale was seen on April 9. Our analyses are limited to a shorter season described below that includes the vast majority of sightings.

Figure 1 summarizes the visual and acoustic data used in our analyses. The horizontal dimension of this figure is time, which is indexed by hour on the bottom axis and calendar date on the top axis. The dual axes are for convenience: the two axes match and either may be used everywhere in the figure. The top portion of the plot shows the acoustic data. Only data within the aperture zone not excluded for data quality reasons are shown (see Figure 2). Each point corresponds to one acoustic location at a particular time and a particular distance from the ice edge. The shaded vertical stripes are times when the recordings were analyzed to estimate locations (blue). About 28% of the analyzed season was examined. The bottom portion of the plot shows the visual data. Counts of sighted whales are summarized by a (upside-down) histogram. The histogram bins are 6 hours wide. The shaded vertical stripes correspond to periods with qualifying watch effort from the primary perch (red). About 45% of the analyzed season was covered with qualifying primary perch effort (see Section 3.1). Only sightings made from the primary perch during these times are counted in the abundance estimate. When the histogram bin edges extend outside the shaded stripes, it should be understood that all the sightings within the bin occurred within the stripe.

2.1 Acoustic Data

The acoustic data are used to estimate the proportion of whales that migrate within visual range. This analysis provides an important correction factor for the total abundance estimate. The nature of the data is that whale calls are converted to estimated spatial locations and corresponding heuristic 95% confidence regions using the methods of Clark et al. (2013). Hereafter, we refer to the data as 'acoustic locations'.

[1]George et al. (2013) explain the distinction between New and Conditional sightings, which we revisit later.

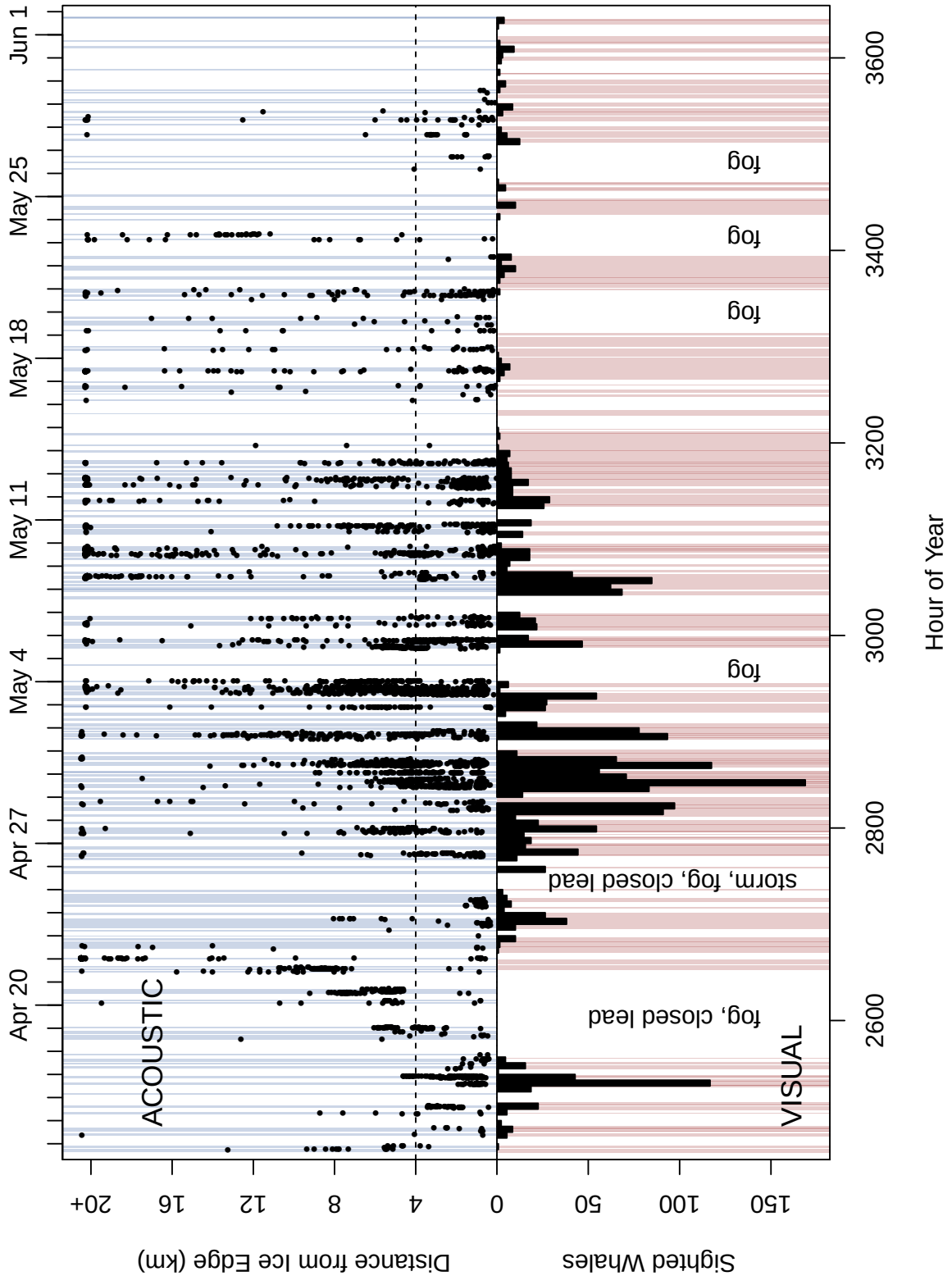

Figure 1: Summary of visual and acoustic data used in our analyses. The top portion plots individual acoustic locations by time and distance from ice edge. The bottom portion shows a (upside-down) histogram of sightings. The vertical stripes correspond to time periods where data are available and white regions correspond to periods without data. See Section 2 for more details.

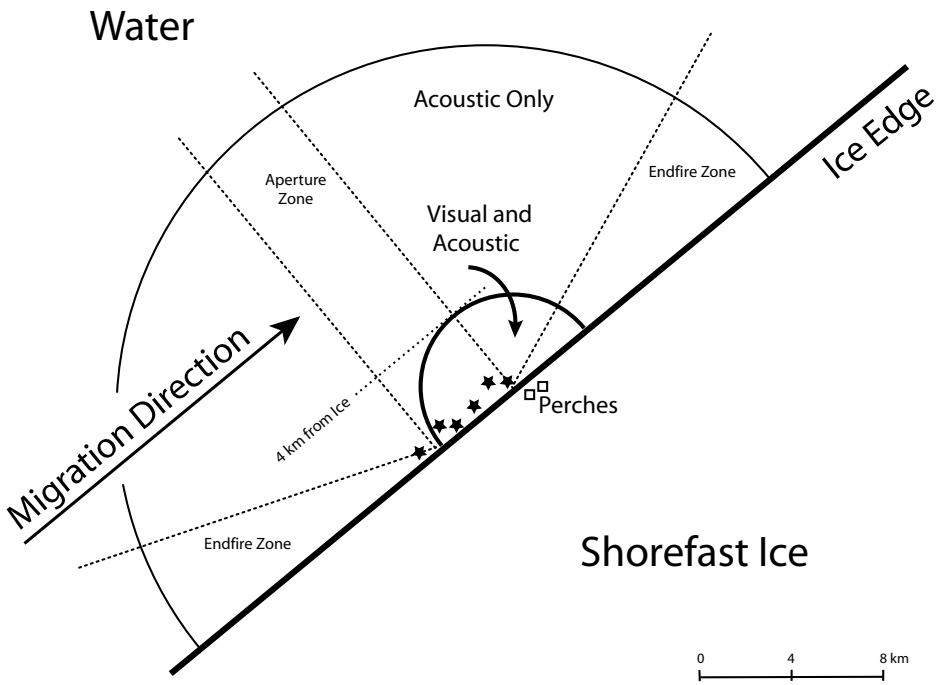

Figure 2: Layout of the 2011 visual and acoustic survey. The six acoustic recorders are stars and the two visual perches are squares. See the text for a full description. This diagram is only a sketch: for precise scale and orientation information see Clark et al. (2013).

During the season, six underwater acoustic recorders were deployed near the ice edge. Clark et al. (2013) describe the details. Figure 2 sketches the survey layout. Although this figure is only roughly scaled and oriented, true north is towards the top and the ice edge is represented by a line that runs from southwest to northeast. Migration proceeds roughly parallel to the ice edge. The two perches are shown as small squares, and the six acoustic recorders are stars.

The larger semicircle in Figure 2 is 20 km from the array centroid. When an acoustic location was estimated to be more than 20 km offshore, the offshore distance was set equal to 20 km. This was done because the estimator was considered to provide a very imprecise (and large) distance for such cases, even though the bearing estimate would be reliable. The array axis is defined by the line between the southwestern-most and northeastern-most recorders. The region within 30 degrees of the array axis and beyond the ends of the array is called the endfire zone. Locations in the endfire zone produce highly uncertain distance estimates due to the geometry involved, and those data are discarded.

The north-easternmost and southwestern-most recorders also determine the aperture of the acoustic array. Roughly, the array aperture is defined to be the segment of the array axis between the ends of the array. The actual southwestern end of the aperture does not extend quite that far for technical reasons (Clark et al., 2013). The two parallel dotted lines that extend the aperture outward, perpendicular to the ice edge, define a strip called the aperture zone. Data within the aperture zone play an important role in the analysis below.

There are three slightly different notions of the 'ice edge'. First is the actual nonlinear contour where the water meets the shorefast ice. Second is the array axis. Since two additional recorders were added partway through the season, there were actually two different array axes. Third is the line connecting the two recorders deployed partway through the season. Unlike the earlier recorders deployed by boat, these two were dropped from the ice edge. Thus, the line between them defines another notion of the ice edge. For further explanation of these concepts, see Clark et al. (2013).

For our purposes, we ignore the distinction between these ice edge definitions. The slight misalignments between these artificial lines and the real ice edge are ignorable because, inter alia, the difference is small within the aperture itself and the real ice edge is not perfectly linear anyway. For the purposes of analysis, the third definition above is the one used to compute offshore distances for the acoustic dataset.

The smaller semicircle in Figure 2 is 4 km from the perches. This represents the practical limit of visual range, and only the sightings within this range are analyzed to estimate detection probability (Givens et al., 2012) and abundance (here). Although this semicircle is unrelated to the acoustic survey, it is shown in the figure to facilitate later discussions.

2.2 Visual Data

The visual survey data have been used to estimate the probability of detecting a whale or group given that it is present (Givens et al., 2012). They also provide the counts that are the foundation of our total abundance estimate.

George et al. (2013) explain the details of the visual survey. Briefly, two visual observation perches were erected on a pressure ridge on the shore-fast ice near the water edge. The perches were 39.4 meters apart, which was sufficiently distant that observers on one perch operated wholly independently from those on the other. The south perch was designated primary, and we attempted to staff it with rotating teams of at least 3 observers at all times, except as limited by safety concerns and weather. The north perch was staffed intermittently for periods of 'independent observer' (IO) effort. Figure 3 shows when each perch was operational.

For the purpose of analysis, the 2011 visual census is defined to have begun at 14:35 local time on April 13, 2011, and ended at 16:00 on June 1, 2011. These are, respectively, the beginning of the first watch session (from the primary perch) and the end of the last one during which a whale was seen. Many of our plots display data by hours of the year; in these units the season ran from 2462.583 to 3640.

3 Methods

3.1 Overview

Visual sightings data refer to groups of whales, although 83% of these groups were size 1. The groups are conceived as being defined when they pass the perches. Group size uncertainty and transitory memberships are accounted for in the detection probability analysis (Givens et al., 2012). Denote the unknown total population size as N. Let us write $N = \sum_{i=1}^{G} c_i$ where the c_i represent group sizes for groups indexed by $i = 1, \ldots, G$.

Let $\delta_i = 1$ if the ith group is seen by observers, and $\delta_i = 0$ otherwise. The total number of whales seen by observers is therefore $n = \sum_{i=1}^{G} \delta_i c_i$ and the total number of observed groups is

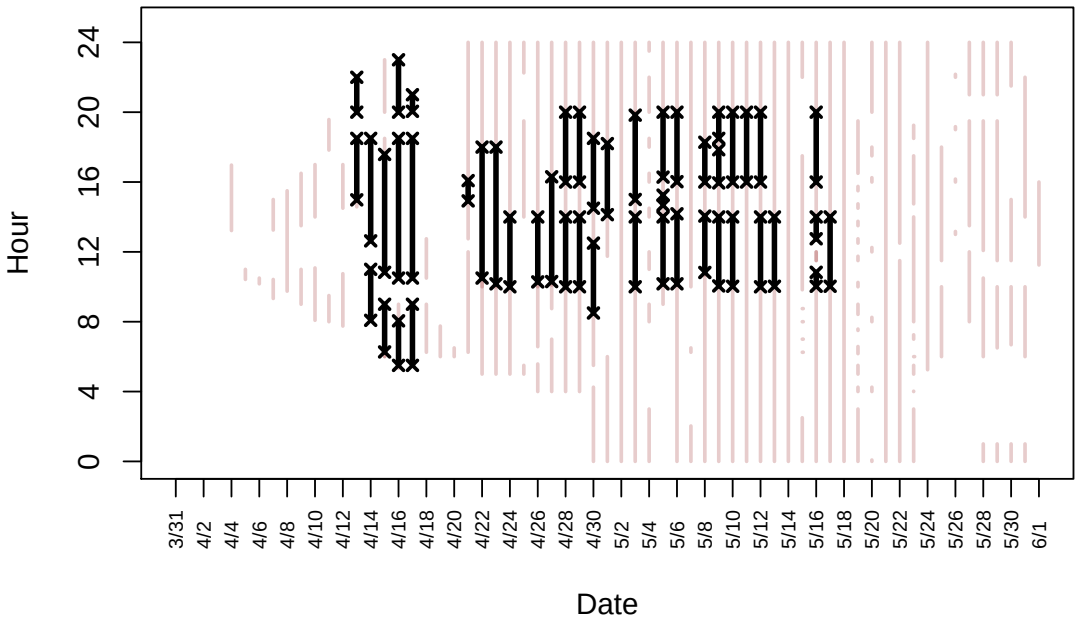

Figure 3: Effort for 2011 visual survey. Black lines represent time with 2-perch IO effort. The boundaries of these periods are indicated with an 'x'. Gray (or red) lines indicate periods when only the primary perch was used. Effort during periods when only binoculars were used have been removed from the figure.

$g = \sum_{i=1}^{G} \delta_i$.

In the remainder of the paper our indexing of the counts c_i is contextual ($i = 1, \ldots, g$ for sighted groups or $i = 1, \ldots, G$ for all groups). In other words, we use the same notation'c_i' to represent counts without adding the notational complexity necessary to keep the subscripting consistent across the two contexts. The intent will be obvious in every case. In our expressions for estimated abundance, we use only the counts from the primary perch; see Section 5 for discussion of this.

Whales are very difficult to see beyond 4 km, although some sightings can be made if visibility conditions are nearly perfect. Our analysis assumes that bowheads are only available to be seen by observers when they swim within the 4 km radius visual detection zone. More distant sightings are ignored in the analysis. Let a_i denote the probability that the ith group was available. If the group is available for visual detection, it may or may not actually be seen from the primary perch. Define the detection probability p_i to be the conditional probability that the ith group was seen given that it was available. Let $\widehat{a}_i$ and $\widehat{p}_i$ denote estimators for a_i and p_i.

During some portions of the season, there was no observer effort because the perch was not staffed, visibility was poor or unacceptable, or the lead was closed (i.e., no open water). Let $S = 1177.417$ denote the total number of hours during the season (i.e., from hour 2462.583 to 3640), and let W denote the total number of those hours for which observer watch effort was maintained during qualifying conditions. Since $W < S$, the abundance estimator must correct for periods of missed survey effort.

Our abundance estimator employs a scaled modified Horvitz-Thompson approach (Borchers

et al., 2002; Horvitz and Thompson, 1952). Informally, the abundance estimate is

$$\widehat{N} = \left\{ \begin{array}{c} \text{correction for} \\ \text{missed effort} \end{array} \right\} \sum_{i=1}^{g} \frac{c_i}{\text{correction for } a_i \text{ and } p_i}. \tag{1}$$

For some past years, bowhead abundance has been estimated using an approach called N_4/P_4 (George et al., 2004). The number of whales passing within a 4 km radius visual detection zone is termed N_4. The total abundance estimate is obtained by dividing an estimate of N_4 by an estimate of the proportion of whales swimming within the visual zone, termed P_4. Those authors estimated detection probabilities and P_4 over blocks of time, then estimated N_4 separately for each day, finally summing the daily totals and correcting for missed effort.

Due to changes in survey design, increased acoustic sampling and improved analytic methods, we do not exactly replicate the N_4/P_4 approach. Our abundance estimate retains the same general philosophy, except that the detection probability and availability correction factors are estimated for each individual whale rather than for large temporal blocks. Conceptually, we replace the estimate of N_4 with the set of $c_i/\widehat{p}_i$, and we replace the estimate of P_4 with the set of $\widehat{a}_i$. Although the methods used to implement this change are necessarily different than previous approaches, we have intentionally tried to avoid changing the principles of those earlier analyses. For example, our definitions of visual and acoustic range, detection and availability, and so forth are the same.

3.2 Detection probability estimation

Givens et al. (2012) describe estimation of the p_i. This approach and the results were reviewed by the IWC Scientific Committee in 2011 and 2012.

Those authors apply a weighted Huggins (1989) model to capture-recapture data from a two-perch independent observer experiment. A critical component of their analysis is matching, i.e., the determination of whether a whale seen at one perch was the same individual as a sighting from the other perch. This process is described by George et al. (2012) and Givens et al. (2012), but is not relevant to the analyses in this paper beyond its contribution to detection probability estimation.

The estimation approach models the ith group as having a detection probability p_i. Then the conditional probability of sighting the group only at the primary perch is $p_i(1-p_i)/d_i$ where $d_i = 1-(1-p_i)^2$ is used because the model is conditioned on seeing the group at least once (since we have no data about unseen whales). The probability of sighting the group only at the second perch is the same, and the probability of sighting the group at both perches is p_i^2/d_i.

Several covariates are recorded along with each sighting. We can express these data in a (transposed) model matrix $\mathbf{X}$ with the ith column $\mathbf{X}_i$ corresponding to the ith sighting. After excluding data from the worst two visibility categories, the only covariates that significantly affected p_i in 2011 were distance of the sighting from the perch, lead condition, and number of whales in the group. A generalized linear model is used to model the dependence:

$$\log\left\{\frac{p_i}{1-p_i}\right\} = \mathbf{X}_i^T\boldsymbol{\beta} \tag{2}$$

where $\boldsymbol{\beta}$ is a parameter column vector to be estimated. Estimated detection probability for a sighting, $\widehat{p}_i$, is derived from the parameter estimates:

$$\widehat{p}_i = \frac{\exp\{\mathbf{X}_i^T\widehat{\boldsymbol{\beta}}\}}{1+\exp\{\mathbf{X}_i^T\widehat{\boldsymbol{\beta}}\}}. \tag{3}$$

Givens et al. (2012) used a weighted estimation method, extending the basic model to account for three uncertainties:

- Some sightings at one occasion may be unintentional resightings of a group already seen at the same occasion ('Conditional' whales).
- The identification of a recapture is uncertain and is given a confidence rating. When a recapture is falsely declared, the constituent data actually comprise two non-recaptured sightings.
- Sightings do not enjoy equal opportunity to be discovered as recaptures because the process of identifying matching whales lacks data on potential matching sightings during periods when the second observer team was not operating.

Despite these additional complexities, the logit-linear model for detection probabilities remains as equation (2). A weighted fit to the model yields parameter estimates $\widehat{\boldsymbol{\beta}}$ and the asymptotic result

$$\widehat{\boldsymbol{\beta}} \sim N(\boldsymbol{\beta}, \boldsymbol{\Phi}). \tag{4}$$

An estimate of the covariance matrix $\boldsymbol{\Phi}$ is obtained as part of fitting the detection probability model; denote this $\widehat{\boldsymbol{\Phi}}$. See Givens et al. (2012) for further details of the detection probability analysis.

3.3 Availability estimation

We use acoustic location data to estimate the a_i. The raw acoustic data are filtered to exclude the endfire regions, locations whose 95% confidence intervals for bearing extend greater than 22.5 degrees from the corresponding point estimate, rare location estimates falling on the grounded ice or land, and locations identified during additional pre-processing by Clark et al. (2013) as very likely being additional calls from the same whale. Here we examine only locations within the array aperture zone, at any distance from the ice edge (see Figure 2). Only these data are displayed in Figures 1 and 6.

These data include offshore distances d_i (meters) and times t_i for $i = 1, \ldots, L$ total locations. Each point is assigned a binary outcome b_i that equals 1 if $d_i \leq 4000$ and 0 otherwise. Clark et al. (2013) describe how a confidence region is estimated for each location, and how this is converted to a confidence interval for each d_i.

We use these confidence intervals to calculate a weight w_i for each b_i. Specifically, we assign to each location a normal distribution, centered at d_i, with variance corresponding to the calculated confidence interval. We then define $w_i = \big|P[d_i < 4000] - 0.5\big|$. Thus the weights are intended to be proportional to the probability that b_i is correct considering the inherent variability in the location estimates.

Our goal is to estimate the proportion of whales that are available to be visually detected within visual range. To be available, the whale must surface at least once within the 4 km semicircle in Figure 2. Conceptually, we estimate this by examining the proportion of acoustic locations inside the aperture zone that are within 4 km of the ice edge. The boundaries of the aperture zone are designated in Figure 2 by the two long dotted parallel lines passing through the array ends and perpendicular to the ice edge. These lines define a strip, and the innermost 4 km of this strip defines a rectangular box where whales may swim through the visual detection zone. Graphically,

our estimate compares the numbers of acoustic locations in this box to whales in the entire strip. In concept, this comparison is the same one used by George et al. (2004).

Our use of the acoustic data and the aperture zone relies on several assumptions. We assume that "on average, the number of locations at any distance is proportional to the number of whales passing at that distance" (George et al., 2004, p. 762). Note that this does not imply that each whale is represented by only a single call in the dataset, although Clark et al. (2013) attempted to remove duplicates as much as possible. We also assume that calling behavior does not systematically vary with distance offshore or vary between whales in any way that would bias estimation of the a_i.

A whale just less than 4 km from the ice edge has some nonzero probability of passing through the aperture zone yet never surfacing in the visual detection zone, since nearest 4 km of the aperture zone is a box but the visual detection zone is semicircular. In fact, every whale has some chance of doing this if it can hold its breath long enough. In a Monte Carlo experiment not described here, we simulated whales and their swim rates, swim angles, dive times and frequencies, offshore distances, and other aspects of bowhead migratory behavior to assess the frequency with which $b_i = 1$ but the whale never surfaced in the visual detection zone. Over a variety of simulation scenarios, we found that the frequency of such cases was about 2%. Therefore, we ignore this complexity hereafter and treat b_i as the availability indicator. This decision will introduce a slight downward bias in our final population abundance estimate.

We adopt a weighted quasi-binomial generalized additive model (GAM) for the b_i data (Wood, 2004, 2006, 2011). The model was fit using the `mgcv` package in the **R** computing language (R Development Core Team, 2012). Letting $a_i = P[b_i = 1]$, we model

$$\log\left\{\frac{a_i}{1-a_i}\right\} = f_a(t_i) \tag{5}$$

where f_a is a penalized regression spline formed from a thin plate regression spline basis, which is the default in the `mgcv` package. The model fitting employed our weights w_i. The number of knots was set at k=20, which allows good fidelity to the data at a temporal frequency and resolution consistent with observer opinions about the rate at which the offshore distribution of whales changes, without over-fitting. Also, in a plot of k versus the unbiased risk estimator criterion, there is a clear, abrupt 'knee' at $k = 20$, which we interpret as an empirical indicator of a good choice. The default generalized cross-validation method was used to choose the smoothness penalty.

This model can be re-expressed in terms of the underlying spline basis functions. Let $\mathbf{Z}$ represent the (transposed) model matrix fashioned from the basis, with one row per basis function and the ith column $\mathbf{Z}_i$ corresponding to the ith case. Then we may write the model as

$$\log\left\{\frac{a_i}{1-a_i}\right\} = \mathbf{Z}_i^T \boldsymbol{\alpha} \tag{6}$$

where $\boldsymbol{\alpha}$ is a column vector of parameters. Fitting equation (5) amounts to estimating $\widehat{\boldsymbol{\alpha}}$. The asymptotic distribution of the parameter estimates $\widehat{\boldsymbol{\alpha}}$ can be summarized by

$$\widehat{\boldsymbol{\alpha}} \sim N(\boldsymbol{\alpha}, \boldsymbol{\Psi}). \tag{7}$$

Technically, this is a limiting Bayesian posterior distribution, but no prior information about $\boldsymbol{\alpha}$ or the a_i is incorporated in the analysis beyond the smoothness penalty; see Wood (2006). A covariance matrix estimate $\widehat{\boldsymbol{\Psi}}$ is obtained while fitting this generalized additive model.

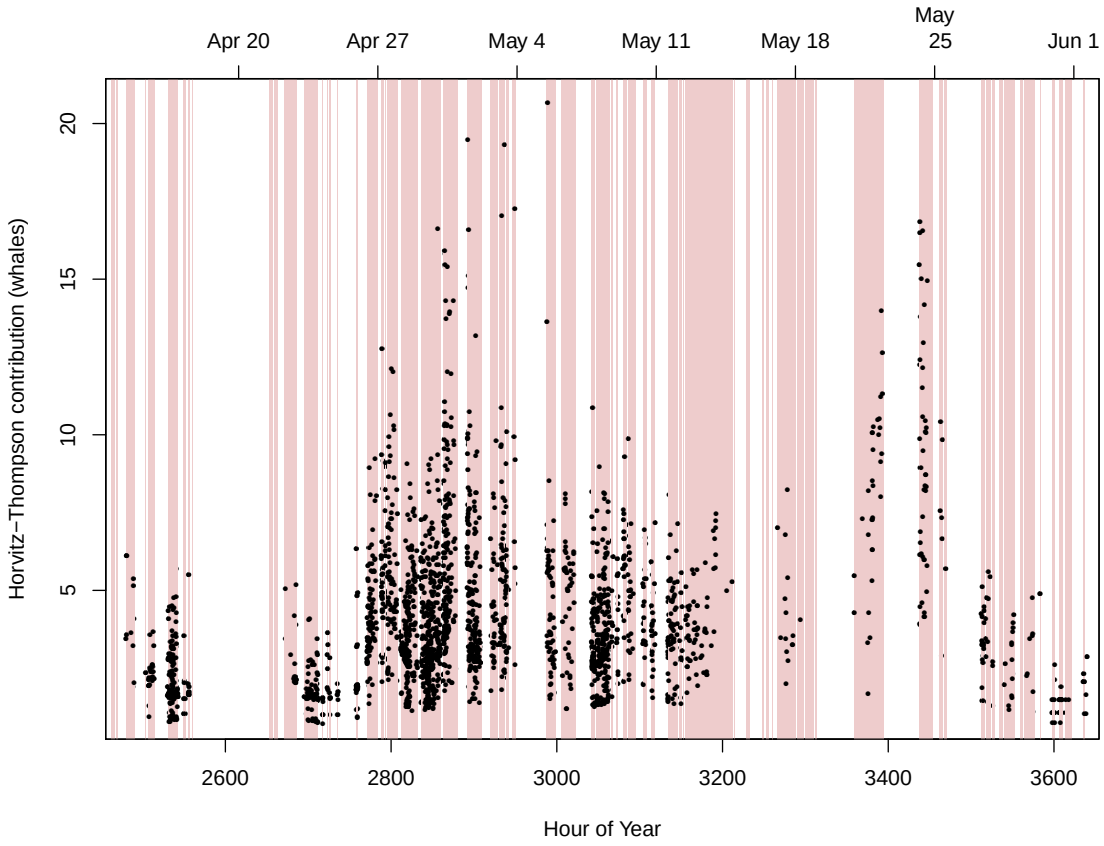

Figure 4: Horvitz-Thompson contribution, h_i, of each sighting (units are whales). The shaded bars correspond to periods of qualifying visual effort.

3.4 Effort estimation

Figure 1 shows the periods of visual effort during the season during qualifying visibility and lead conditions. To correct for periods without effort, it does not suffice to add up missed clock time—we must account also for the passage rate of whales during the missed periods.

To do this, we begin by recalling from equation (1) that $\widehat{N}$ involves a sum of terms

$$h_i = c_i/\{\text{correction for } a_i \text{ and } p_i\},$$

which we call Horvitz-Thompson contributions. The exact form of these h_i is explained in Section 3.5. The h_i represent the estimated number of whales that the ith sighting contributes to the overall abundance estimate (unscaled by effort). Figure 4 plots the Horvitz-Thompson contributions against time during the season. Note that whale abundance is symbolized in this plot by *both* the density of points and the magnitudes of individual points.

Let $f_r(t)$ denote the passage rate of whales past the census area, so that the total number of whales passing the perch at any distance, detected or unseen, between time t_1 and t_2 is $\int_{t_1}^{t_2} f_r(t)dt$.

Let S and W denote the sets of time periods corresponding to the total analyzed survey season and periods of qualifying watch effort, respectively. Then the proportion of the total population passing Barrow during the season that passed during periods of qualifying watch effort is

$$E = \int_W f_r(t)dt \Big/ \int_S f_r(t)dt \tag{8}$$

and the desired correction factor in the conceptual estimator of abundance in equation (1) is $1/E$. This approach relies on the assumption that passage rate does not depend on observer presence. We also assume that the model of a smoothly varying passage rate curve over all periods of the day is reasonable.

To estimate f_r and hence E, we bin the h_i into 12-hour time blocks, $\mathcal{B}_1, \ldots, \mathcal{B}_{101}$ and define H_j to equal the sum of all h_i that occurred during block $\mathcal{B}_j$. Thus, H_j is the total Horvitz-Thompson contribution for the jth block, i.e., an estimate of the total number of whales passing during that block during times of qualifying effort. Let T_j denote the amount of qualifying watch effort during the jth block and let the blocks be referenced by their temporal midpoints t_j. Then define $R_j = H_j/T_j$ to be the block passage rate: the number of passing whales per qualifying watch hour.

We adopt a quasi-Poisson generalized additive model with log link to model the block passage rates according to $R_j \sim \text{Poisson}(\lambda_j)$ and

$$\log \lambda_j = f_r(t_j) \tag{9}$$

where f_r is a smooth passage rate function. We use the same GAM fitting tools and technical assumptions as previously used for modeling availability. Points are weighted proportionally to the T_j.

This model can be re-expressed in terms of a matrix $\mathbf{U}$ with one row per spline basis function and the jth column representing the jth block, using

$$\log \lambda_j = \mathbf{U}_j^T \boldsymbol{\gamma}. \tag{10}$$

The column vector of parameter estimates $\widehat{\boldsymbol{\gamma}}$ has a limiting posterior distribution

$$\widehat{\boldsymbol{\gamma}} \sim N(\boldsymbol{\gamma}, \boldsymbol{\Lambda}) \tag{11}$$

in the same sense as above. The covariance matrix estimate $\widehat{\boldsymbol{\Lambda}}$ is estimated during model fitting.

Having obtained an estimated smooth function $\widehat{f_r}$ in this way, what remains is to estimate E. We set

$$\widehat{E} = \int_W \widehat{f_r}(t)dt \Big/ \int_S \widehat{f_r}(t)dt \tag{12}$$

where the integrals are approximated using Simpson's rule (e.g., Givens and Hoeting 2013).

Let $\widehat{\text{var}}\{1/\widehat{E}\}$ denote the estimated variance of the correction factor estimator $1/\widehat{E}$. We estimate the variance using the parametric bootstrap approach recommended by Wood (2006, p. 202-3). Briefly, the GAM is first fit to the original data, then bootstrap iterations proceed as follows. Using the estimated mean function from the original fitted model, bootstrap response data are generated from the parametric (Poisson) model. A new GAM is fit to these data to obtain a bootstrap estimate of the smoothing parameter. Next, a GAM is fit to the original data using the bootstrap smoothing parameter value. This produces one set of estimates $\widehat{\boldsymbol{\gamma}}^*$ and $\widehat{\boldsymbol{\Lambda}}^*$. We

performed 2000 bootstrap iterations. Then, to simulate from the bootstrap distribution of $1/\widehat{E}$, we may select at random one of the 2000 distributions $N(\widehat{\boldsymbol{\gamma}}^*, \widehat{\Lambda}^*)$ and sample a value $\boldsymbol{\gamma}^{**}$ from it. This value is used to obtain a bootstrap value $\widehat{E}^*$ via equation (12). Finally, the sample variance of the values of $1/\widehat{E}^*$ is computed to produce $\widehat{\text{var}}\{1/\widehat{E}\}$.

Note that $1/\widehat{E}$ and its variance estimator are not statistically independent of the other key estimators ($\widehat{a}_i$, $\widehat{p}_i$ and $\widehat{\theta}_i$) in this paper. However, the nature of $\widehat{E}$ as an integral of a smooth function of the huge set of those quantities renders this inconsequential: it is very reasonable to treat $\widehat{E}$ as independent of our other estimators for our purposes.

3.5 Abundance estimation

We write the total abundance estimate as $\widehat{N} = \widetilde{N}/\widehat{E}$ where $\widetilde{N}$ is the estimated total abundance of animals passing during times of observer (visual) effort, and $1/\widehat{E}$ is the estimated effort correction factor. Define

$$\theta_i = \frac{1}{a_i p_i} \tag{13}$$

and let $\widehat{\theta}_i$ denote an estimator for θ_i. Then

$$\widehat{N} = \frac{\widetilde{N}}{\widehat{E}} = \frac{1}{\widehat{E}} \sum_{i=1}^{G} \delta_i c_i \widehat{\theta}_i = \frac{1}{\widehat{E}} \sum_{i=1}^{g} c_i \widehat{\theta}_i. \tag{14}$$

using only the counts c_i from the primary perch. Since

$$\widetilde{N} = \sum_{i=1}^{g} c_i \widehat{\theta}_i \tag{15}$$

the distributions of $\widetilde{N}$ and $\widehat{N}$ depend on the distribution of the $\widehat{\theta}_i$, and hence on $\widehat{\boldsymbol{\beta}}$ and $\widehat{\boldsymbol{\alpha}}$.

In this section, we describe the major points of the abundance estimation method. Our point estimate, $\widetilde{N}$, is a Horvitz-Thompson type estimator (Borchers et al., 2002; Horvitz and Thompson, 1952). The abundance estimator and its theoretical mean and variance are derived as extensions to the results of Steinhorst and Samuel (1989). Our approach to variance estimation extends that of Wong (1996); see also Fieberg (2012). It provides an asymptotically unbiased variance estimator to replace the more familiar biased estimator of Steinhorst and Samuel (1989). The full technical justification our approach and derivation of our mathematical results are postponed to the appendix.

We begin with consideration of the θ_i. As shown in the appendix,

$$\widehat{\theta}_i = (1 + \exp\{-\widehat{\mu}_i - \phi_i/2\})\,(1 + \exp\{-\widehat{\eta}_i - \psi_i/2\}) \tag{16}$$

$$\tag{17}$$

is asymptotically unbiased for $\widehat{\theta}_i$, where

$$\begin{aligned} \widehat{\mu}_i &= \mathbf{X}_i^T \widehat{\boldsymbol{\beta}} \\ \widehat{\eta}_i &= \mathbf{Z}_i^T \widehat{\boldsymbol{\alpha}} \\ \phi_i &= \mathbf{X}_i^T \widehat{\boldsymbol{\Phi}} \mathbf{X}_i \\ \psi_i &= \mathbf{Z}_i^T \widehat{\boldsymbol{\Psi}} \mathbf{Z}_i. \end{aligned}$$

The result that

$$\mathbb{E}\,\widehat{\theta}_i = \theta_i \tag{18}$$

asymptotically follows from properties of the lognormal distribution and treating $\widehat{\mathbf{\Phi}} = \mathbf{\Phi}$ and $\widehat{\mathbf{\Psi}} = \mathbf{\Psi}$ as known for large samples. This treatment of covariance matrices is why we do not place hats on ϕ_i and ψ_i. We also use the fact that $\widehat{\theta}_i$ and $\widehat{\eta}_i$ are independent because they arise from parameter estimates $\widehat{\boldsymbol{\beta}}$ and $\widehat{\boldsymbol{\alpha}}$ which are estimated from two entirely separate datasets. If $\widehat{\boldsymbol{\beta}}$, $\widehat{\boldsymbol{\alpha}}$, $\widehat{\mathbf{\Phi}}$, and $\widehat{\mathbf{\Psi}}$ are consistent estimators, then so are the estimators discussed here.

We estimate the variance of $\widehat{\theta}_i$ using

$$\begin{aligned}
\widehat{\mathrm{var}}\{\widehat{\theta}_i\} &= \exp\{-2\widehat{\mu}_i - 2\phi_i\}\,(1 + 2\exp\{-2\widehat{\mu}_i - \widehat{\eta}_i - 2\phi_i - \psi_i\})\,(\exp\{\phi_i\} - 1) + \\
&\quad \exp\{-2\widehat{\eta}_i - 2\psi_i\}\,(1 + 2\exp\{-\widehat{\mu}_i - 2\widehat{\eta}_i - \phi_i - 2\psi_i\})\,(\exp\{\psi_i\} - 1) + \\
&\quad \exp\{-2\widehat{\mu}_i - 2\widehat{\eta}_i - 2\phi_i - 2\psi_i\}\,(\exp\{\phi_i + \psi_i\} - 1)\,.
\end{aligned} \tag{19}$$

We show in the appendix that

$$\mathbb{E}\,\widehat{\mathrm{var}}\{\widehat{\theta}_i\} = \mathrm{var}\{\widehat{\theta}_i\} \tag{20}$$

asymptotically. Similarly, the estimator

$$\begin{aligned}
\widehat{\mathrm{cov}}\{\widehat{\theta}_i, \widehat{\theta}_j\} &= K_\phi \left(\exp\{-\widehat{\mu}_i - \widehat{\mu}_j - \widetilde{\phi}_{ij}\}\right)(1 + \exp\{-\widehat{\eta}_i - \psi_i/2\} + \exp\{-\widehat{\eta}_j - \psi_j/2\}) + \\
&\quad K_\psi \left(\exp\{-\widehat{\eta}_i - \widehat{\eta}_j - \widetilde{\psi}_{ij}\}\right)(1 + \exp\{-\widehat{\mu}_i - \phi_i/2\} + \exp\{-\widehat{\mu}_j - \phi_j/2\}) + \\
&\quad (\exp\{\phi_{ij} + \psi_{ij}\} - 1)\exp\{-\widehat{\mu}_i - \widehat{\mu}_j - \widehat{\eta}_i - \widehat{\eta}_j - \widetilde{\phi}_{ij} - \widetilde{\psi}_{ij}\}
\end{aligned} \tag{21}$$

where

$$\begin{aligned}
K_\phi &= (\exp\{\phi_{ij}\} - 1) \\
K_\psi &= (\exp\{\psi_{ij}\} - 1) \\
\phi_{ij} &= \mathbf{X}_i^T \widehat{\mathbf{\Phi}} \mathbf{X}_j \\
\psi_{ij} &= \mathbf{Z}_i^T \widehat{\mathbf{\Psi}} \mathbf{Z}_j. \\
\widetilde{\phi}_{ij} &= \phi_i/2 + \phi_j/2 + \phi_{ij} \\
\widetilde{\psi}_{ij} &= \psi_i/2 + \psi_j/2 + \psi_{ij}
\end{aligned} \tag{22}$$

can be shown to be asymptotically unbiased:

$$\mathbb{E}\,\widehat{\mathrm{cov}}\{\widehat{\theta}_i, \widehat{\theta}_j\} = \mathrm{cov}\{\widehat{\theta}_i, \widehat{\theta}_j\}. \tag{23}$$

These variance and covariance estimators are necessary for estimating the variance of the abundance estimator.

The appendix proves that

$$\widehat{\mathrm{var}}\{\widetilde{N}\} = \widehat{V}_1 + \widehat{V}_2 \tag{24}$$

is an asymptotically unbiased estimator of $\mathrm{var}\{\widetilde{N}\}$, where

$$\begin{aligned}
\widehat{V}_1 &= \sum_{i=1}^{g} c_i^2 \left(\widehat{\theta}_i^2 - \widehat{\theta}_i - \widehat{\mathrm{var}}\{\widehat{\theta}_i\}\right) \\
\widehat{V}_2 &= \sum_{i=1}^{g} c_i^2 \widehat{\mathrm{var}}\{\widehat{\theta}_i\} + \sum_{i \neq j}^{g} \sum c_i c_j \widehat{\mathrm{cov}}\{\widehat{\theta}_i, \widehat{\theta}_j\}.
\end{aligned}$$

In Section 3.4 we described how to estimate the variance of $1/\widehat{E}$ and the justification for treating $\widehat{E}$ and $\widetilde{N}$ as independent. Now since

$$\widehat{N} = \widetilde{N} \Big/ \widehat{E} \tag{25}$$

we can estimate the variance of $\widehat{N}$ as the variance of the product of independent random variables:

$$\widehat{\text{var}}\{\widehat{N}\} = \frac{1}{\widehat{E}^2}\widehat{\text{var}}\{\widetilde{N}\} + \widetilde{N}^2\widehat{\text{var}}\{1/\widehat{E}\} + \widehat{\text{var}}\{\widetilde{N}\}\widehat{\text{var}}\{1/\widehat{E}\}. \tag{26}$$

Wong (1996) has demonstrated (for a simpler case than ours) that it is better to estimate a confidence interval by applying a normal approximation to log abundance and then back-transforming the result. If we define $\widehat{CV}^2 = \widehat{\text{var}}\{\widehat{N}\}/\widehat{N}^2$, the 95% confidence interval for N is

$$\left(\widehat{N}\exp\{-1.96\widehat{CV}\},\ \ \widehat{N}\exp\{1.96\widehat{CV}\}\right). \tag{27}$$

We adopt that strategy in this paper.

The counts c_i we use for this abundance estimate include both New sightings (whales definitely seen for the first time) and Conditional sightings (whales seen a second time from the same perch and observers are unsure whether the whale has been previously seen). Previous abundance estimates have always treated Conditional whales as half a whale each; we continue that tradition here.

The counts also include some sightings made only with binoculars. Note that about half of the whales are initially spotted with binoculars, at which point the observers use a theodolite to record bearing and vertical angle data from which whale location can be estimated. About 10% of the time, no theodolite sighting is obtained due to the absence of the device or an operator, or the failure to find the whale with the device despite binocular detection. Unfortunately, such 'binocular-only' data do not provide sufficiently precise estimates of range for our analyses, and the detection probability p_i cannot be estimated for these sightings. Like George et al. (2004), we do not exclude these cases. When the detection probability is not available we can scale the sighting by $1/\widehat{a}_i$ while setting $\widehat{p}_i = 1$. This corrects for the proportion of whales swimming beyond visual range while making no correction for detectability. Note that this approach is conservative because we know that for every whale, $a_i \leq 1$ and $p_i < 1$. Therefore, the partial corrections described here will scale up the sighting less than any full correction would. For this reason, the abundance estimator will be lower than if a complete correction was available.

An estimate of a_i is not available for two sightings outside the time period of the season we have defined. We included these cases by setting a_i equal to the mean of the season.

We do not include whales seen only at perch 2. The reason for this is explained in Section 5.

3.6 Trend estimation

The N_4 and P_4 estimates summarized by Zeh and Punt (2005) for 11 years between 1978 and 2001 comprise a valuable time series from which we may estimate population rate-of-increase, or trend. An independent abundance estimate for 2004 based on photo-id data is not included because it does not produce N_4 and P_4 estimates. To estimate the trend, we replicate the method previously used for this population (Cooke, 1996; Punt and Butterworth, 1999; George et al., 2004; Zeh and Punt, 2005).

The surveys between 1978 and 2001 are correlated because they share information about availability: the P_4 values for certain years are used to make abundance estimates for other years when

no separate estimate of P_4 is available. The approach we describe here accounts for the resulting correlation. It is a two-step procedure.

The first step is to estimate indices of abundance for all years when N_4 estimates are available (regardless of whether a corresponding P_4 is available). This estimation proceeds by fitting a model having three components. First, each observed log abundance is assumed to equal the sum of the true total log abundance in that year, the log proportion of the population within visual range in that year, and an independent normal error. Second, each observed log proportion within visible range is assumed to equal the sum of the corresponding true log proportion within visible range for that year and an independent normal error. Third, the true log proportion within visible range is assumed to equal a grand mean log proportion plus normal error. The second and third components introduce interannual process error. The overall model combining these three components is fit by restricted maximum likelihood. It is important to stress that the resulting abundance indices are not considered to be the 'official' abundance estimates for the corresponding years. Rather, they are indices created to 'share information' about P_4 for years in which no P_4 was directly estimated.

The second step of the process is to estimate trend using the fitted abundance indices. The trend can be estimated by fitting an exponential growth model using generalized least squares, incorporating the variance-covariance matrix of log abundances estimated in step 1 as the weighting matrix. A confidence interval for the trend estimate is calculated using asymptotic results.

Incorporating our new 2011 estimate into this procedure is not entirely straightforward because our approach does not estimate the quantities P_4 and N_4. To obtain N_4, we replicated the entire analysis in this paper, ignoring the a_i factors. This provides an estimate of total abundance that is not corrected for the proportion of whales swimming within 4 km of the perch. Additional technical details about this analysis are given in the appendix. George et al. (2004) define P_4 to be "the proportion of the acoustic locations directly offshore from the hydrophone array that fall within 4 km offshore from the perch" (p. 761). We compute this proportion and estimate its variance using a block bootstrap, where the blocks are chosen to be the discrete acoustic sampling periods (e.g., Givens and Hoeting 2013).

4 Results

4.1 Detection probabilities

The detection probability estimates of Givens et al. (2012) are shown in Figure 5. Let r_i, ℓ_i and s_i denote the distance, lead condition and group size for the ith sighting, respectively, and define $I(s_i = 1) = 1$ for group sizes equaling 1 (a single whale) and 0 otherwise. Similarly, let $I(\ell_i =$ 'wide open') and $I(\ell_i =$ 'patchy') indicate specific lead conditions. Then the 2011 detection probabilities p_i are modeled as

$$\text{logit}\{p_i\} = \beta_0 + \beta_1 r_i + \beta_2 I(s_i = 1) + \beta_3 I(\ell_i = \text{'patchy'}) + \beta_4 I(\ell_i = \text{'wide open'}). \qquad (28)$$

Data with lead conditions of 'wide open', 'continuous', and 'patchy' were used to fit the model and the effect of 'continuous' leads is subsumed into the intercept. 'Poor' and 'unacceptable' visibility sightings and binocular sightings were excluded from this analysis. Table 1 shows parameter estimates for this model and Table 2 gives the corresponding covariance matrix of the estimates, namely $\widehat{\mathbf{\Phi}}$.

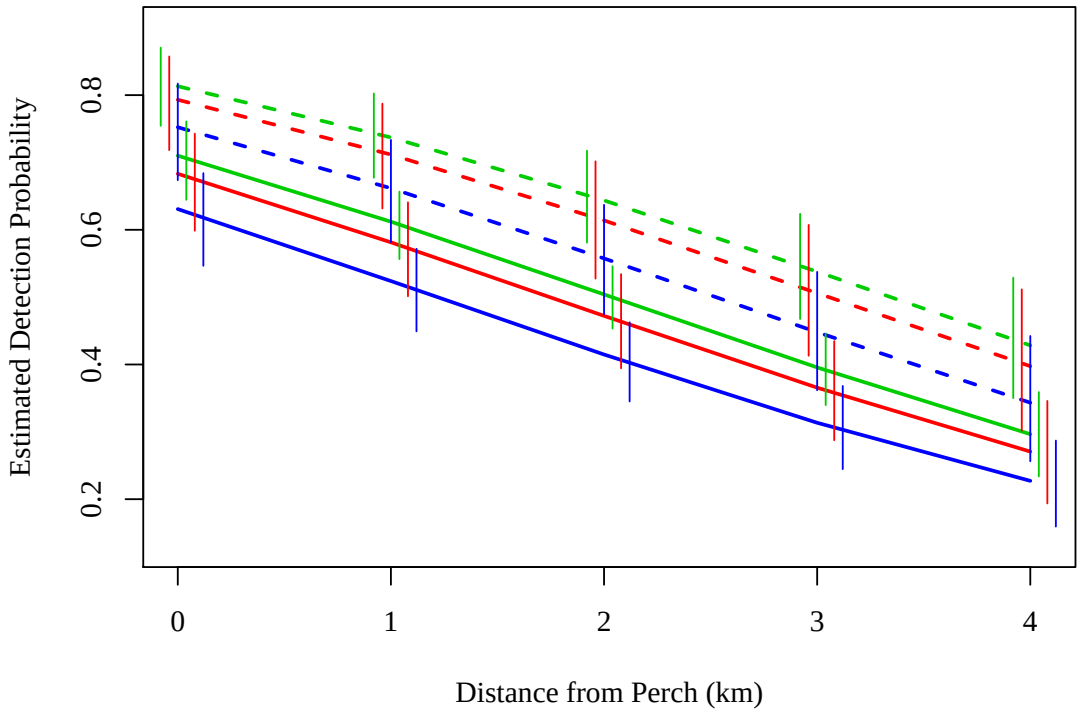

Figure 5: Estimated detection probabilities from the analysis of Givens et al. (2012) for the 2011 visual survey. Solid lines correspond to single animals; dotted lines are for larger groups. For each line style, there are 3 colors: continuous leads (green), patchy leads (red), and wide open water (blue). In black and white, these are in the same top-to-bottom order for both single animals and groups. Individual 95% confidence intervals for the estimates are shown as vertical lines at integer km distances, but horizontally offset so they can be distinguished.

Table 1: Parameter estimates for the model of 2011 detection probabilities.

$\widehat{\beta}_0$	$\widehat{\beta}_1$	$\widehat{\beta}_2$	$\widehat{\beta}_3$	$\widehat{\beta}_4$
1.4712	-0.0004399	-0.5752	-0.1274	-0.3603

Table 2: Variance-covariance matrix for $(\widehat{\beta}_0, \widehat{\beta}_1, \widehat{\beta}_2, \widehat{\beta}_3, \widehat{\beta}_4)$ from estimation of the 2011 detection probabilities.

3.790553e-03	-6.968852e-07	-2.071643e-03	-9.416339e-04	-1.052317e-03
	3.334503e-10	6.295729e-08	8.984788e-08	1.107493e-07
		2.453591e-03	-3.181631e-05	5.646251e-05
			2.766833e-03	8.217309e-04
				2.190653e-03

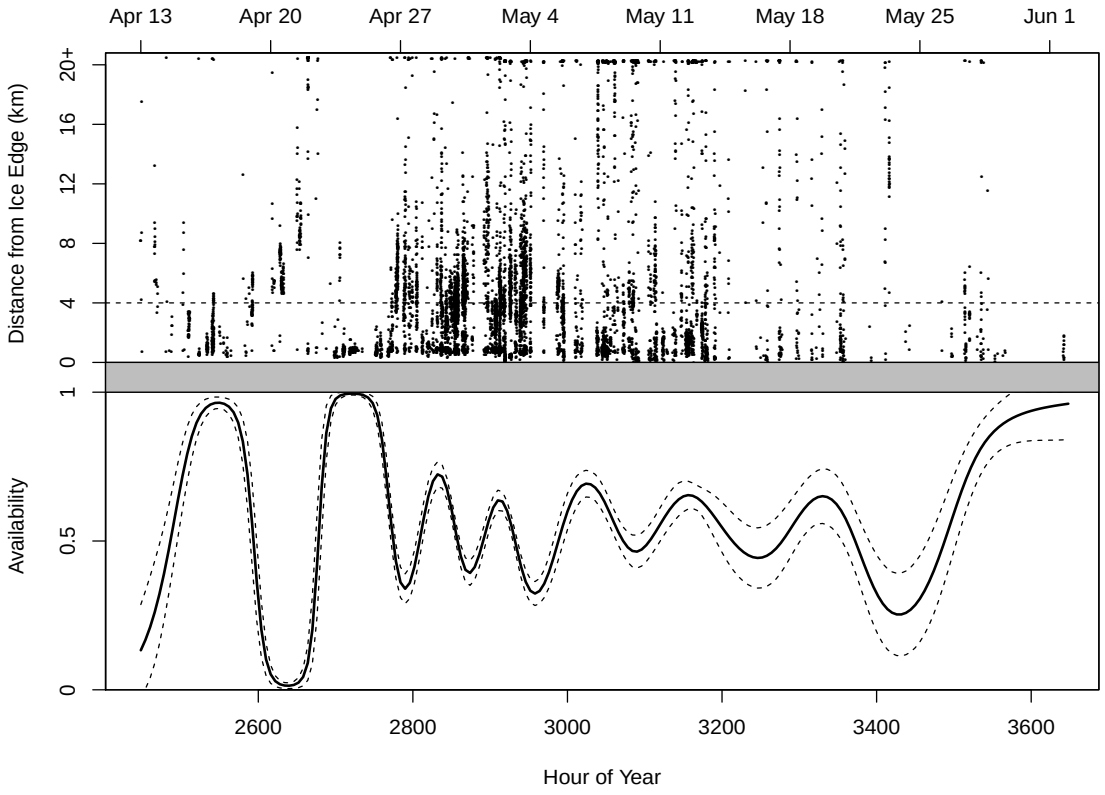

Figure 6: The bottom panel shows the estimate and 95% confidence bounds for the availability $\text{logit}^{-1}\widehat{f}_a(t)$ over the course of the season. Recall that availability is defined to be the probability that a whale swims within 4 km of the ice edge and is estimated from only the acoustic data. The top panel shows the raw acoustics data: each point represents one acoustic location at a specific time and distance from the ice edge. When whales are far offshore, they are not available to be seen by observers.

4.2 Availability

Figure 6 shows the estimated availability curve, $\widehat{f}_a(t)$. The top panel of this figure displays one point for each acoustic location in the same manner as Figure 1. Availability is defined to be the probability that a whale swims within 4 km of the ice edge, and is fit with a spline on the logit scale; see equation (5). The solid line in the bottom panel is the fitted curve on the probability scale, i.e., $\exp\{\widehat{f}_a(t)\}/(1+\exp\{\widehat{f}_a(t)\})$. The dotted lines correspond to 95% pointwise confidence intervals for each time. Averaging across time, the mean availability is 0.581; averaging across whales it is 0.619.

Although this fitted curve looks quite wiggly and spans a large range of probabilities, the time span covered by this graph is 50 days, so the temporal variation in availability is not as rapid as it may appear. Further, the rate of variation is consistent with observer impressions of migratory behavior, and slower than what can be caused by changes in ice conditions. The very large amount of acoustic data allows us to reliably estimate $f_a(t)$ at this temporal resolution.

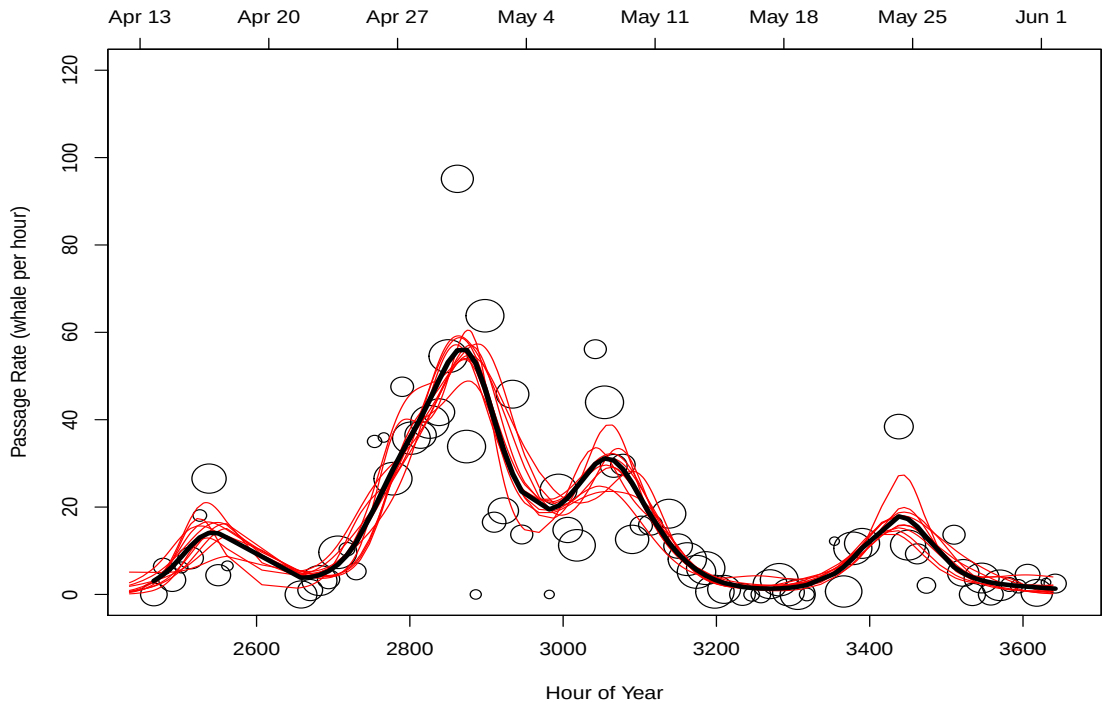

Figure 7: Estimated passage rate, $\exp\{\widehat{f}_r(t)\}$. Block passage rates R_j (whales/hour) are shown with the circles, with area proportional to T_j. The fit to these points using the quasi-Poisson GAM spline is shown with the the heavy line. Ten bootstrap replicates are also shown.

4.3 Effort

The estimation of effort is based on the individual Horvitz-Thompson contributions h_i $(i = 1, \ldots, g)$ and their block totals H_j $(j = 1, \ldots, 101)$. Figure 4 plots the h_i against time. Recall that the value of h_i is a number of whales, and that overall whale density and passage rate are determined by *both* the density of dots and the individual magnitudes of the h_i. The periods of qualifying visual effort are indicated by the shaded bars.

Figure 7 consolidates these data as described in Section 3.4. The total Horvitz-Thompson contribution for the jth twelve-hour block is divided by the amount of qualifying watch effort during the block to create an hourly passage rate $R_j = H_j/T_j$ for $j = 1, \ldots, 101$. Figure 7 plots the R_j using one circle per block. The area of a circle is proportional to T_j (which are used as weights for fitting). The heavy curve is the (back-transformed) spline fit for the passage rate, i.e. $\exp\{f_r(t)\}$. Also shown with thinner (red) lines are 10 random block bootstrap pseudo-fits.

Figure 8 a histogram of the 2000 bootstrap estimates $\widehat{E}^*$, which is roughly symmetric and centered on the point estimate of 0.520 with a bootstrap standard error of 0.015, yielding a correction factor of $1/\widehat{E} = 1.921$ with a bootstrap standard error of 0.055.

4.4 Abundance

The point estimate of $\widetilde{N}$, uncorrected for effort, is equal to the sum of the Horvitz-Thompson contributions, i.e., the sum of the h_i values in Figure 4. This is 8,971 whales. Adjusting for qualifying effort yields the fully corrected abundance estimate $\widehat{N} = 16,892$.

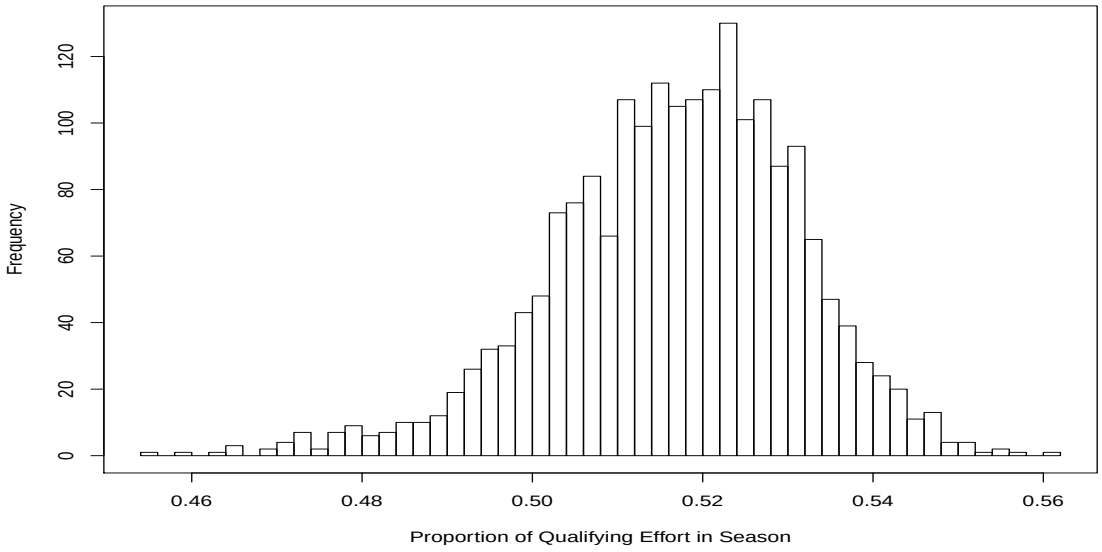

Figure 8: Histogram of block bootstrap estimates $\widehat{E}^*$, the proportion of the season with qualifying visual effort.

Variance calculations yield $\widehat{V}_1 = 184.85^2$, $\widehat{V}_2 = 398.73^2$ and $\widehat{\text{var}}\{\widetilde{N}\} = 439.50^2$. Applying equation (26) to incorporate variability due to the effort correction yields $\widehat{\text{var}}\{\widehat{N}\} = 975.40^2$. Thus, the confidence interval for the estimate is (15,074, 18928).

4.5 Trend

The results are shown in Figure 9. Each abundance index is represented by its point estimate (dot) and 95% confidence interval (vertical line). The estimated exponential growth model (curve) indicates an annual rate of increase of 3.7% with a 95% confidence interval of (2.8%, 4.7%).

A pointwise 95% confidence band is also shown. This was obtained by drawing samples from the joint asymptotic distribution of the fitted parameter estimates, constructing the corresponding fitted curves, and calculating pointwise quantiles.

5 Discussion

Here we address some choices made during the analysis. We also examine our results in a broader context.

5.1 Exclusion of perch 2 data

Both our estimators ignore the 340 whales seen only at perch 2. The reason for this is that including these sightings as random variables would require a change to the definition of detection, which in turn would greatly complicate variance estimation.

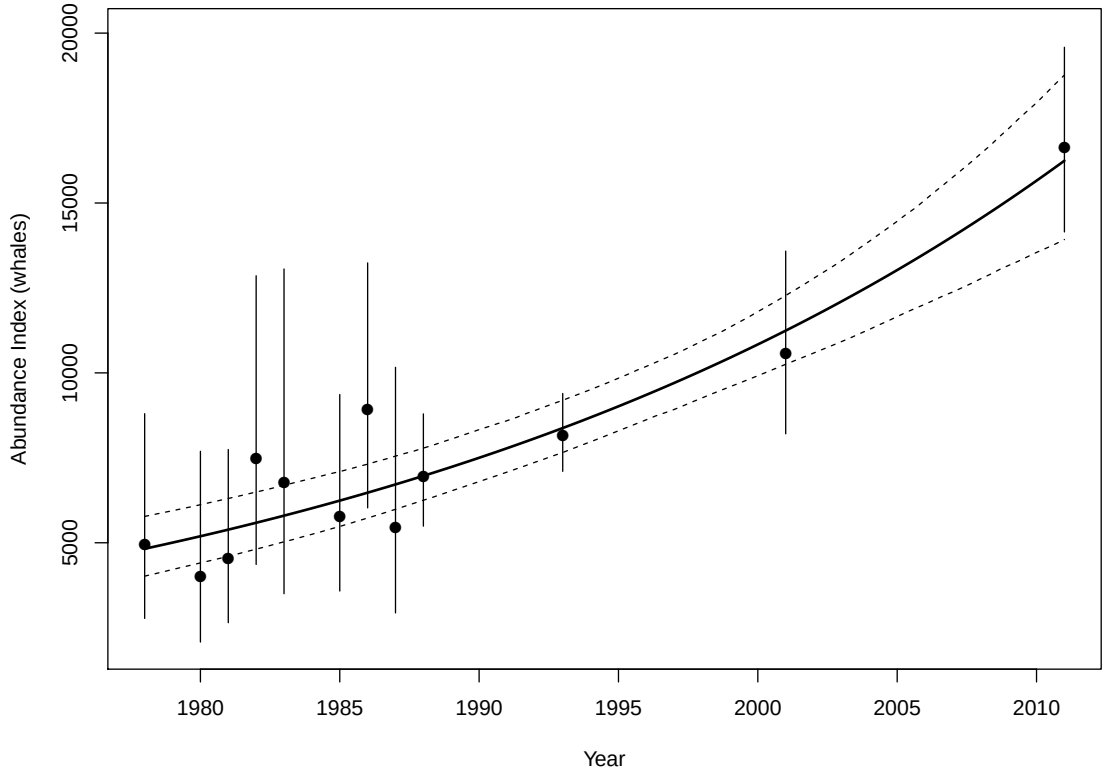

Figure 9: Estimated abundance indices, fitted curve, and pointwise 95% confidence band for the trend estimate using the time series from 1978–2011.

If we were to include these whales, the detection probability portion of the Horvitz-Thompson correction would need to represent $P[\text{seen from at least one perch}] = 1 - (1 - p_i)^2$ when IO is operational and $P[\text{seen at perch 1}] = p_i$ when it is not (Borchers et al., 1998). This differs from our current approach that uses only the primary perch data and the corresponding probabilities p_i. The change would introduce a quadratic function of p_i into θ_i and the denominator of the abundance estimator. For variance estimation we would need to consider expectations of exponentiations of squares of normal random variables. Compensating for this is possible, however the estimators and proofs of their asymptotic properties would be more complicated. It is not clear that the approach would make a substantial difference. We defer consideration of this alternative as a topic for possible future research.

5.2 Bias and variance results

Our approach treats $\widehat{\mathbf{\Phi}}$ and $\widehat{\mathbf{\Psi}}$ as if they are the true values of the corresponding covariance matrices. The adequacy of this approximation has been simulation tested in a wide range of scenarios (Wong, 1996). Generally, the results showed good bias and variance performance, even with sample sizes nearly 20 times smaller than ours. We conclude that the approximation used here has negligible impact on the results.

5.3 Whales migrating outside the analyzed season

Anecdotal evidence suggests that our estimate excludes some periods when whales passed Barrow. Although the first bowhead was seen on April 9, our analyzed season does not begin until April 13. During this period, a few whales were seen during sporadic effort with poor to fair visibility. In recent years, we have seen a surprising number of whales pass Barrow very early in the season (including before April 9), and the limited evidence we have from 2011 suggests that this phenomenon continues.

Acoustic recording continued after June 1, when the visual survey was ended due to safety concerns caused by degrading ice. No systematic sampling of the post-season acoustic data has been done. However, casual inspection of a few hours of data after June 1 indicates that calls still occur. Most times, call rates appear to be much lower than typical days during the visual survey season. However, there are brief periods (e.g., a two-hour block on June 2) where a large number of calls are detected. After June 15, few calls were found. An acoustic survey in 2009 found over 2000 bowhead calls in 13 hours of sampling after June 1 (BRP, 2010). The number of whales producing these vocalizations is highly uncertain, however, because the vocalization pattern of an individual bowhead ranges from a single call to up to 400 calls per hour (Zeh et al., 1993)[2].

These sources of evidence suggest that some whales—perhaps a significant number—passed Barrow outside the analyzed season in 2011. Since we have ignored these whales in our analysis, this omission is a source of downward bias in the total abundance estimate.

5.4 Comparison with past work

The most recent abundance estimate is 12,631 in 2004 (95% CI (7,900, 19,700)) from photo-identification work (Koski et al., 2010). The most recent ice-based visual survey estimate is 10,545 in 2001 (95% CI (8,200, 13,500)) and the estimated rate-of-increase for 1978-2001 is 3.4% (1.7%, 5%) (Zeh and Punt, 2005). Our estimate for 2011 is consistent with these estimates (Figure 9). In other words, our new abundance estimate is about what would have been expected before conducting the 2011 survey. The new estimate of trend has a narrower confidence interval because a new point has been added to the abundance time series. The uncertainty estimates for the 2011 abundance estimate are comparable to those for some of the best previous estimates.

Givens et al. (2012) note that their estimated 2011 detection probabilities are somewhat lower on average than estimates for other years, and a bit less dependent on sighting distance. The 2011 standard errors are considerably smaller due to larger sample sizes and improved methodology. These tendencies would favor a larger and more precise abundance estimate.

Using data from 1978-1985, Zeh and Punt (2005) estimate the interannual mean P_4 to be 0.701, compared to our time-averaged 2011 mean of 0.581. For eight years between 1979 and 2001, Zeh and Punt (2005) estimate P_4 to be 0.405, 0.479, 0.567, 0.740, 0.750, 0.850, 0.862, and 0.933 (sorted). Clearly the interannual variation is considerable. Our estimate for 2011 is not unusual, although perhaps a bit lower than average and much lower than the largest past values. Low availability values produce higher abundance estimates.

In 2011, there were 50 days from the date when the first whale in the analyzed season was seen until watch effort ended. For 11 previous seasons when N_4 has been estimated, the median is 47

[2]Recall that the acoustic data used in our analysis have been filtered to remove such duplicate calls (Clark et al., 2013).

with a range from 30 to 55. In 2011, the total number of hours of watch of any kind (including poor and unacceptable visibility) at the primary perch in the analyzed season was 859. The median of the past seasons is 996 with a range from 448 to 1130 hours. Perhaps the two most successful past seasons, 1993 and 2001, are most comparable to 2011. These had season days of 49 and 54, and watch hours of 1067 and 1130. These numbers illustrate that the 2011 effort was not exceptional by either standard.

The estimated standard error of our abundance estimate is slightly smaller than for some historical estimates. This is particularly noticeable when expressed as a CV since the 2011 abundance estimate is the largest ever. One reason for the reduced uncertainty is that the survey benefited from relatively consistent good viewing conditions during the season. There were no long periods without effort. This limits the variability of the estimated passage rate curve and hence the $\widehat{E}$ correction factor. The variance of the detection probability estimates has also been reduced compared to past years due to improved methodology. Finally, we simply have an unprecedentedly large amount of data: over 4,000 New and Conditional whale sightings and over 22,000 acoustic locations.

Finally, it is important to look at the big picture. In this section we have described ways in which our results differ a bit from past results. The overall impression, however, is that these differences are quite small compared to the interannual variation in such estimates and our findings are not unusual or surprising considering what we have seen over the last 30 years.

5.5 Management implications

Indigenous hunting quotas for this population are recommended using the Bowhead Strike Limit Algorithm (SLA). This procedure was adopted by the IWC after rigorous simulation testing covering a wide range of trial scenarios (International Whaling Commission, 2003). An important consideration in that testing was the population increase rate, both in terms of the theoretical maximum sustainable yield rate (MSYR) and the empirical trend estimate.

The rate-of-increase estimate following the 2001 survey was 3.4% (1.7%, 5%) (Zeh and Punt, 2005). Our updated rate-of-increase estimate is 3.7%, which is wholly consistent with the past estimate and has lower confidence bound (2.8%) further above zero than for 2001. This suggests that the range of values of MSYR considered during Bowhead SLA trials continues to be appropriate. If anything, our new results indicate that the larger trial values of MSYR were likely more plausible than the lowest. Bowhead SLA performance on trials with medium and high MSYR values was extremely good.

At the time that the Bowhead SLA was adopted, the most recent abundance estimate was 10,545 in 2001 (95% CI (8,200, 13,500)). Our new estimate for 2011 is 16,892 (95% CI (15,074, 18,928)). Clearly the population size has continued to grow substantially under the Bowhead SLA quotas since 2003, and there is no evidence that the population size is above the maximum net productivity level or near carrying capacity.

We conclude that the 2011 abundance and trend results provide no reason to question the suitability of the Bowhead SLA. If anything, these results provide greater evidence that the Bowhead SLA will meet IWC conservation goals than had previously been understood.

Acknowledgments

This work was supported by the National Oceanic and Atmospheric Administration (via a major grant through the Alaska Eskimo Whaling Commission (AEWC)) and the North Slope Borough (Alaska) Department of Wildlife Management. We thank the many observers, matchers, and other colleagues who conducted this challenging survey with amazing tenacity and professionalism often under dangerous field conditions. We also acknowledge the cooperation of the AEWC and thank BP Alaska for providing additional funding for field logistics. We also thank the whale hunters of Barrow who supported our studies and allowed us to conduct survey operations near their camps on the sea ice. Bailey Fosdick is thanked for helpful discussions on availability estimation. Taqulik Hepa, Harry Brower, Dolores Vinas and Molly Spicer from the North Slope Borough and Johnny Aiken and Jessica Lefevre from the AEWC are thanked for their organizational and administrative support. Finally, Judith Zeh is thanked for her advice and wisdom about virtually every aspect of the bowhead surveys over 30 years.

References

Borchers, D., Buckland, S., Goedhart, P., Clarke, E., and Hedley, S. (1998). Horvitz-Thompson estimators for double-platform line transect surveys. *Biometrics*, 54:1221–1237.

Borchers, D., Buckland, S., and Zucchini, W. (2002). *Estimating Animal Abundance: Closed Populations*. Springer Verlag.

BRP (2010). Passive acoustic monitoring of spring bowhead whale migration, Point Barrow, Alaska, 9 April - 9 June 2009. Technical Report 10-15 by the Bioacoustics Research Program of the Cornell Lab of Ornithology, Ithaca, NY, for the Dept. of Wildlife Management, North Slope Borough, Alaska. 17pp.

Clark, C., Charif, R., Hawthorne, D., Rahaman, A., Givens, G., George, J., and Muirhead, C. (2013). Analysis of acoustic data from the spring 2011 bowhead whale census at Point Barrow, Alaska. Paper SC/65a/BRG09 presented to the Scientific Committee of the International Whaling Commission, June, 2013.

Cooke, J. G. (1996). Preliminary investigation of an RMP-based approach to the management of aboriginal subsistence whaling. Paper SC/48/AS5 presented to the IWC Scientific Committee, June, 1996.

Fieberg, J. R. (2012). Estimating population abundance using sightability models: R SightabilityModel package. *Journal of Statistical Software*, 51.

George, J., Givens, G., Suydam, R., Herreman, J., Tudor, B., DeLong, R., Mocklin, J., and Clark, C. (2013). Summary of the spring 2011 ice-based visual, aerial photo-ID, and acoustic survey of bowhead whales near Point Barrow, Alaska. Paper SC/65a/BRG11 presented to the Scientific Committee of the IWC, June 2013.

George, J., Herreman, J., Givens, G., Suydam, R., Mocklin, J., Clark, C., Tudor, B., and DeLong, R. (2012). Brief overview of the 2010 and 2011 bowhead whale abundance surveys near Point Barrow, Alaska. Paper SC/64/AWMP7 presented to the IWC Scientific Committee, June 2012.

George, J. C., Zeh, J., Suydam, R., and Clark, C. (2004). Abundance and population trend (1978-2001) of the western Arctic bowhead whales surveyed near Barrow, Alaska. *Marine Mammal Science*, 20:755–773.

Givens, G. H., Edmondson, S. L., George, J. C., Tudor, B., DeLong, R. A., and Suydam, R. (2012). Detection probability estimates from the 2011 ice-based independent observer surveys of bowhead whales near Barrow, Alaska, using a weighted recapture model. Paper SC/65a/BRG01 submitted to the Scientific Committee of the International Whaling Commission, June 2012.

Givens, G. H. and Hoeting, J. A. (2013). *Computational Statistics, Second Edition*. John Wiley and Sons, Inc., Hoboken, NJ. 469pp.

Horvitz, D. and Thompson, D. (1952). A generalization of sampling without replacement from a finite universe. *Journal of the American Statistical Association*, 47:663–685.

Huggins, R. (1989). On the statistical analysis of capture experiments. *Biometrika*, 76:133–140.

International Whaling Commission (2003). Chair's report of the fifty-fourth annual meeting. Annex C. Report of the aboriginal subsistence whaling sub-committee. *Ann. Rep. Int. Whaling Comm.*, 2002:62–75.

Koski, W., Zeh, J., Mocklin, J., Davis, A., Rugh, D., George, J., and Suydam, R. (2010). Abundance of Bering-Chukchi-Beaufort bowhead whales (*Balaena mysticetus*) in 2004 estimated from photo-identification data. *Journal of Cetacean Research and Management*, 11:89–99.

Punt, A. E. and Butterworth, D. S. (1999). On assessments of the Bering-Chukchi-Beaufort Seas stock of bowhead whales (*Balaena mysticetus*) using a Bayesian approach. *Journal of Cetacean Research and Management*, 1:53–71.

R Development Core Team (2012). *R: A Language and Environment for Statistical Computing*. R Foundation for Statistical Computing, Vienna, Austria. ISBN 3-900051-07-0.

Steinhorst, K. R. and Samuel, M. D. (1989). Sightability adjustment methods for aerial surveys of wildlife populations. *Biometrics*, 45:415–425.

Wong, C.-N. (1996). *Population size estimation using the modified Horvitz-Thompson estimator with estimated sighting probability*. PhD thesis, Colorado State University, Department of Statistics.

Wood, S. N. (2004). Stable and efficient multiple smoothing parameter estimation for generalized additive models. *Journal of the American Statistical Association*, 99:673–686.

Wood, S. N. (2006). *Generalized Additive Models: An Introduction with R*. Chapman & Hall/CRC, Boca Raton, FL.

Wood, S. N. (2011). Fast stable restricted maximum likelihood and marginal likelihood estimation of semiparametric generalized linear models. *Journal of the Royal Statistical Society, Series B*, 73:3–36.

Zeh, J., Clark, C., George, J., Withrow, D., Carroll, G., , and Koski, W. (1993). Current population size and dynamics. In Burns, J., Montague, J., and Cowles, C., editors, *The Bowhead Whale*, pages 409–489. Special Publication No. 2 of the Society for Marine Mammaology, Lawrence, KS.

Zeh, J. and Punt, A. (2005). Updated 1978-2001 abundance estimates and their correlations for the Bering-Chukchi-Beaufort Seas stock of bowhead whales. *Journal of Cetacean Research and Management*, 7:169:175.

Appendix: Statistical Results

Abundance Estimate

Recall that the total abundance estimate is $\widehat{N} = \widetilde{N}/\widehat{E}$ where $\widetilde{N}$ is the estimated total abundance of animals passing during times of observer effort, and $1/\widehat{E}$ is the estimated effort correction factor. Define

$$\theta_i = \frac{1}{a_i p_i} \tag{29}$$

and let $\widehat{\theta}_i$ denote an estimator for θ_i. Then

$$\widehat{N} = \frac{\widetilde{N}}{\widehat{E}} = \frac{1}{\widehat{E}} \sum_{i=1}^{G} \delta_i c_i \widehat{\theta}_i = \frac{1}{\widehat{E}} \sum_{i=1}^{g} c_i \widehat{\theta}_i \tag{30}$$

using the notation of Section 3, including that $\delta_i = 1$ if the ith group is sighted (and zero otherwise) so $\mathbb{E}\,\delta_i = 1/\theta_i$. Since

$$\widetilde{N} = \sum_{i=1}^{g} c_i \widehat{\theta}_i, \tag{31}$$

the distributions of $\widetilde{N}$ and $\widehat{N}$ depend on the distribution of the $\widehat{\theta}_i$, and hence on the parameter estimates $\widehat{\boldsymbol{\beta}}$ and $\widehat{\boldsymbol{\alpha}}$ from the models in equations (2) and (6).

Using the logit link relationships in our availability and detection probability models, properties of the lognormal distribution, the asymptotic normality of $\widehat{\boldsymbol{\beta}}$ and $\widehat{\boldsymbol{\alpha}}$, and the approximation that $\boldsymbol{\Phi}$ and $\boldsymbol{\Psi}$ can be treated as known for large samples, one can find asymptotically unbiased estimators of all important quantities needed to produce a total abundance estimate. If $\widehat{\boldsymbol{\beta}}$, $\widehat{\boldsymbol{\alpha}}$, $\widehat{\boldsymbol{\Phi}}$ and $\widehat{\boldsymbol{\Psi}}$ are consistent, then so are the estimators discussed below.

The goal of this appendix is to show that $\widehat{N}$ is asymptotically unbiased for N, and to find an asymptotically unbiased estimate of its variance and hence a confidence interval. To do this, we first explore how to estimate $\widetilde{N}$ and its variance.

For notational simplicity, it is useful to define some terms related to the linear predictors and covariance matrices in the generalized additive models for the visual and acoustic data. Specifically, define

$$\begin{aligned}
\widehat{\mu}_i &= \mathbf{X}_i^T \widehat{\boldsymbol{\beta}} \\
\widehat{\eta}_i &= \mathbf{Z}_i^T \widehat{\boldsymbol{\alpha}} \\
\mu_i &= \mathbf{X}_i^T \boldsymbol{\beta} \\
\eta_i &= \mathbf{Z}_i^T \boldsymbol{\alpha} \\
\phi_i &= \mathbf{X}_i^T \widehat{\boldsymbol{\Phi}} \mathbf{X}_i \\
\psi_i &= \mathbf{Z}_i^T \widehat{\boldsymbol{\Psi}} \mathbf{Z}_i \\
\phi_{ij} &= \mathbf{X}_i^T \widehat{\boldsymbol{\Phi}} \mathbf{X}_j \\
\psi_{ij} &= \mathbf{Z}_i^T \widehat{\boldsymbol{\Psi}} \mathbf{Z}_j. \\
\widetilde{\phi}_{ij} &= \phi_i/2 + \phi_j/2 + \phi_{ij} \\
\widetilde{\psi}_{ij} &= \psi_i/2 + \psi_j/2 + \psi_{ij}
\end{aligned} \tag{32}$$

using the notation developed previously in this paper. Note that terms like ϕ_i and ψ_{ij} denote projections and quadratic forms related to the estimated covariance matrices, not individual terms therein. Since we treat these matrices as known, we don't put hats on these expressions. Note that $\phi_{ij} = \phi_{ji}$ and $\psi_{ij} = \psi_{ji}$. Finally, note that $2\widetilde{\phi}_{ij} = (\mathbf{X}_i + \mathbf{X}_j)^T \widehat{\mathbf{\Phi}} (\mathbf{X}_i + \mathbf{X}_j)$ and $2\widetilde{\psi}_{ij} = (\mathbf{Z}_i + \mathbf{Z}_j)^T \widehat{\mathbf{\Psi}} (\mathbf{Z}_i + \mathbf{Z}_j)$.

Now we estimate the correction factor θ_i. We begin by showing that

$$\widehat{\theta}_i \;=\; (1 + \exp\{-\widehat{\mu}_i - \phi_i/2\})\,(1 + \exp\{-\widehat{\eta}_i - \psi_i/2\}) \tag{33}$$

is an asymptotically unbiased estimator for θ_i. Expanding $\widehat{\theta}_i$ as

$$\widehat{\theta}_i = 1 + \exp\{-\widehat{\mu}_i - \phi_i/2\} + \exp\{-\widehat{\eta}_i - \psi_i/2\} + \exp\{-\widehat{\mu}_i - \widehat{\eta}_i - (\phi_i + \psi_i)/2\} \tag{34}$$

we can see that the unbiasedness follows from properties of the lognormal distribution. Specifically, recall that if $Y \sim N(\mu, \sigma^2)$ then $\mathbb{E}\exp\{Y\} = \exp\{\mu + \sigma^2/2\}$ and $\mathrm{var}\{\exp\{Y\}\} = \exp\{2\mu + 2\sigma^2\} - \exp\{2\mu + \sigma^2\}$. Now consider the expectation of the first random component of $\widehat{\theta}_i$ in equation (34):

$$\begin{aligned}
\mathbb{E}\exp\{-\widehat{\mu}_i - \phi_i/2\} &= \exp\{-\phi_i/2\}\,\mathbb{E}\exp\{-\widehat{\mu}_i\} \\
&= \exp\{-\phi_i/2\}\,\mathbb{E}\exp\{-\mathbf{X}_i^T\widehat{\boldsymbol{\beta}}\} \\
&= \exp\{-\phi_i/2\}\,\mathbb{E}\exp\{-\mathbf{X}_i^T\boldsymbol{\beta} + \phi_i/2\} \\
&= \exp\{-\mu_i\}
\end{aligned} \tag{35}$$

since $\widehat{\mu}_i$ is normal because $\widehat{\boldsymbol{\beta}}$ is normal. The other portions of the expectation work out similarly. Combining pieces like this,

$$\begin{aligned}
\mathbb{E}\,\widehat{\theta}_i &= 1 + \exp\{-\mu_i\} + \exp\{-\eta_i\} + \exp\{-\mu_i - \eta_i\} \\
&= (1 + \exp\{-\mu_i\})\,(1 + \exp\{-\eta_i\}) \\
&= \frac{1}{p_i a_i} \\
&= \theta_i
\end{aligned} \tag{36}$$

so the asymptotic unbiasedness of $\widehat{\theta}_i$ has been shown.

Now we derive $\mathrm{var}\{\widehat{\theta}_i\}$. Again concentrating on the first random term in the estimator in equation (34), note that

$$\begin{aligned}
\mathrm{var}\{\exp\{-\widehat{\mu}_i - \phi_i/2\}\} &= \exp\{-\phi_i\}\mathrm{var}\{\exp\{-\widehat{\mu}\}\} \\
&= \exp\{-\phi_i\}\,(\exp\{-2\mu_i + 2\phi_i\} - \exp\{-2\mu_i + \phi_i\}) \\
&= \exp\{-2\mu_i\}\,(\exp\{\phi_i\} - 1)
\end{aligned} \tag{37}$$

recalling that $\exp\{-\widehat{\mu}_i\} \sim \mathrm{lognormal}(-\mu_i, \phi_i)$ and using properties of this distribution. The other variance parts work out similarly. Next, consider the covariance between the first and third random terms in equation (34). Here, we use the property that for constants u and v and random variables R and S, $\mathrm{cov}\{uR, vSR\} = uv(\mathbb{E}\,S)\mathrm{var}\{R\}$. Now

$$\begin{aligned}
&\mathrm{cov}\{\exp\{-\widehat{\mu}_i - \phi_i/2\}, \exp\{-\widehat{\mu}_i - \widehat{\eta}_i - (\phi_i + \psi_i)/2\}\} \\
&\qquad= \exp\{-\phi_i/2\}\exp\{-(\phi_i + \psi_i)/2\}\,(\mathbb{E}\exp\{-\widehat{\eta}_i\})\,\mathrm{var}\{\exp\{-\widehat{\mu}_i\}\} \\
&\qquad= \exp\{-\phi_i - \psi_i/2\}\exp\{-\eta_i + \psi_i/2\}\,(\exp\{-2\mu_i + 2\phi_i\} - \exp\{-2\mu_i + \phi_i\}) \\
&\qquad= \exp\{-2\mu_i - \eta_i\}\,(\exp\{\phi_i\} - 1)\,.
\end{aligned} \tag{38}$$

A key step in this result follows from the fact that $\widehat{\theta}_i$ and $\widehat{\eta}_i$ are independent because they arise from parameter estimates $\widehat{\boldsymbol{\beta}}$ and $\widehat{\boldsymbol{\alpha}}$ which are estimated from two entirely separate datasets. Computing all the relevant variance and covariance terms analogously to equations (37) and (38), one can show

$$\begin{aligned}\mathrm{var}\{\widehat{\theta}_i\} &= \exp\{-2\mu_i\}\left(1+2\exp\{-\eta_i\}\right)\left(\exp\{\phi_i\}-1\right)+\\ &\quad \exp\{-2\eta_i\}\left(1+2\exp\{-\mu_i\}\right)\left(\exp\{\psi_i\}-1\right)+\\ &\quad \exp\{-2\mu_i-2\eta_i\}\left(\exp\{\phi_i+\psi_i\}-1\right).\end{aligned} \tag{39}$$

Deriving the covariance between $\widehat{\theta}_i$ and $\widehat{\theta}_j$ relies on similar lognormal calculations and the independence between visual and acoustic datasets. The result is

$$\begin{aligned}\mathrm{cov}\{\widehat{\theta}_i,\widehat{\theta}_j\} &= \left(\exp\{\phi_{ij}\}-1\right)\left(\exp\{-\mu_i-\mu_j\}\right)\left(1+\exp\{-\eta_i\}+\exp\{-\eta_j\}\right)+\\ &\quad \left(\exp\{\psi_{ij}\}-1\right)\left(\exp\{-\eta_i-\eta_j\}\right)\left(1+\exp\{-\mu_i\}+\exp\{-\mu_j\}\right)+\\ &\quad \left(\exp\{\phi_{ij}+\psi_{ij}\}-1\right)\exp\{-\mu_i-\mu_j-\eta_i-\eta_j\}.\end{aligned} \tag{40}$$

Now we need to find asymptotically unbiased estimates for these quantities. Let us estimate the variance using the estimator

$$\begin{aligned}\widehat{\mathrm{var}}\{\widehat{\theta}_i\} &= \exp\{-2\widehat{\mu}_i-2\phi_i\}\left(1+2\exp\{-2\widehat{\mu}_i-\widehat{\eta}_i-2\phi_i-\psi_i\}\right)\left(\exp\{\phi_i\}-1\right)+\\ &\quad \exp\{-2\widehat{\eta}_i-2\psi_i\}\left(1+2\exp\{-\widehat{\mu}_i-2\widehat{\eta}_i-\phi_i-2\psi_i\}\right)\left(\exp\{\psi_i\}-1\right)+\\ &\quad \exp\{-2\widehat{\mu}_i-2\widehat{\eta}_i-2\phi_i-2\psi_i\}\left(\exp\{\phi_i+\psi_i\}-1\right).\end{aligned} \tag{41}$$

Similar methods to those above can be used to prove

$$\mathbb{E}\,\widehat{\mathrm{var}}\{\widehat{\theta}_i\}=\mathrm{var}\{\widehat{\theta}_i\} \tag{42}$$

asymptotically. Similarly, the estimator

$$\begin{aligned}\widehat{\mathrm{cov}}\{\widehat{\theta}_i,\widehat{\theta}_j\} &= K_\phi\left(\exp\{-\widehat{\mu}_i-\widehat{\mu}_j-\widetilde{\phi}_{ij}\}\right)\left(1+\exp\{-\widehat{\eta}_i-\psi_i/2\}+\exp\{-\widehat{\eta}_j-\psi_j/2\}\right)+\\ &\quad K_\psi\left(\exp\{-\widehat{\eta}_i-\widehat{\eta}_j-\widetilde{\psi}_{ij}\}\right)\left(1+\exp\{-\widehat{\mu}_i-\phi_i/2\}+\exp\{-\widehat{\mu}_j-\phi_j/2\}\right)+\\ &\quad \left(\exp\{\phi_{ij}+\psi_{ij}\}-1\right)\exp\{-\widehat{\mu}_i-\widehat{\mu}_j-\widehat{\eta}_i-\widehat{\eta}_j-\widetilde{\phi}_{ij}-\widetilde{\psi}_{ij}\}\end{aligned} \tag{43}$$

where

$$\begin{aligned}K_\phi &= \left(\exp\{\phi_{ij}\}-1\right)\\ K_\psi &= \left(\exp\{\psi_{ij}\}-1\right)\end{aligned}$$

can be shown to be asymptotically unbiased:

$$\mathbb{E}\,\widehat{\mathrm{cov}}\{\widehat{\theta}_i,\widehat{\theta}_j\}=\mathrm{cov}\{\widehat{\theta}_i,\widehat{\theta}_j\}. \tag{44}$$

We are now able to derive the variance of

$$\widetilde{N}=\sum_{i=1}^{G}\delta_i c_i\widehat{\theta}_i \tag{45}$$

using the conditional variance formula. We obtain

$$\begin{aligned}
\mathrm{var}\left\{\widetilde{N}\right\} &= \mathrm{var}_\delta\left\{\mathbb{E}_{\widehat{\theta}|\delta}\widetilde{N}\right\} + \mathbb{E}_\delta\left\{\mathrm{var}_{\widehat{\theta}|\delta}\widetilde{N}\right\} \\
&= \mathrm{var}_\delta\left\{\sum_{i=1}^{G}\delta_i c_i\,\mathbb{E}_{\widehat{\theta}|\delta}\widehat{\theta}_i\right\} + \mathbb{E}_\delta\left\{\sum_{i=1}^{G}\delta_i^2 c_i^2 \mathrm{var}_{\widehat{\theta}|\delta}\widehat{\theta}_i + \sum\sum_{i\neq j}^{G}\delta_i\delta_j c_i c_j \mathrm{cov}_{\widehat{\theta}|\delta}\{\widehat{\theta}_i,\widehat{\theta}_j\}\right\} \\
&= \sum_{i=1}^{G} c_i^2\theta_i^2\mathrm{var}_\delta\{\delta_i\} + \sum_{i=1}^{G} c_i^2\,\mathbb{E}_\delta\{\delta_i\}\mathrm{var}\{\widehat{\theta}_i\} + \sum\sum_{i\neq j}^{G} c_i c_j\,\mathbb{E}_\delta\{\delta_i\delta_j\}\mathrm{cov}\{\widehat{\theta}_i,\widehat{\theta}_j\} \\
&= \sum_{i=1}^{G} c_i^2\theta_i^2\frac{1}{\theta_i}\left(1-\frac{1}{\theta_i}\right) + \sum_{i=1}^{G}\frac{c_i^2}{\theta_i}\mathrm{var}\{\widehat{\theta}_i\} + \sum\sum_{i\neq j}^{G}\frac{c_i c_j}{\theta_i\theta_j}\mathrm{cov}\{\widehat{\theta}_i,\widehat{\theta}_j\} \\
&= \left[\sum_{i=1}^{G} c_i^2(\theta_i-1)\right] + \left[\sum_{i=1}^{G}\frac{c_i^2}{\theta_i}\mathrm{var}\{\widehat{\theta}_i\} + \sum\sum_{i\neq j}^{G}\frac{c_i c_j}{\theta_i\theta_j}\mathrm{cov}\{\widehat{\theta}_i,\widehat{\theta}_j\}\right] \\
&= V_1 + V_2. \qquad (46)
\end{aligned}$$

Let us define

$$\widehat{V}_1 = \sum_{i=1}^{g} c_i^2\left(\widehat{\theta}_i^2 - \widehat{\theta}_i - \widehat{\mathrm{var}}\{\widehat{\theta}_i\}\right). \qquad (47)$$

Then

$$\begin{aligned}
\mathbb{E}\,\widehat{V}_1 &= \mathbb{E}\sum_{i=1}^{g} c_i^2\left(\widehat{\theta}_i^2 - \widehat{\theta}_i - \widehat{\mathrm{var}}\{\widehat{\theta}_i\}\right) \\
&= \mathbb{E}_\delta\,\mathbb{E}_{\widehat{\theta}|\delta}\left\{\sum_{i=1}^{G}\delta_i c_i^2\left(\widehat{\theta}_i^2 - \widehat{\theta}_i - \widehat{\mathrm{var}}\{\widehat{\theta}_i\}\right)\right\} \\
&= \mathbb{E}_\delta\sum_{i=1}^{G}\delta_i c_i^2\left(\mathbb{E}_{\widehat{\theta}|\delta}\widehat{\theta}_i^2 - \mathbb{E}_{\widehat{\theta}|\delta}\widehat{\theta}_i - \mathbb{E}_{\widehat{\theta}|\delta}\widehat{\mathrm{var}}\{\widehat{\theta}_i\}\right) \\
&= \mathbb{E}_\delta\sum_{i=1}^{G}\delta_i c_i^2(\theta_i^2-\theta_i) \\
&= \sum_{i=1}^{G}\frac{c_i^2}{\theta_i}(\theta_i^2-\theta_i) \\
&= \sum_{i=1}^{G} c_i^2(\theta_i-1) \\
&= V_1 \qquad (48)
\end{aligned}$$

so $\widehat{V}_1$ is asymptotically unbiased for V_1. Since $\widehat{\mathrm{var}}\{\widehat{\theta}_i\}$ and $\widehat{\mathrm{cov}}\{\widehat{\theta}_i,\widehat{\theta}_j\}$ are asymptotically unbiased, we can define

$$\widehat{V}_2 = \sum_{i=1}^{g} c_i^2\widehat{\mathrm{var}}\{\widehat{\theta}_i\} + \sum\sum_{i\neq j}^{g} c_i c_j\widehat{\mathrm{cov}}\{\widehat{\theta}_i,\widehat{\theta}_j\} \qquad (49)$$

as the asymptotically unbiased estimator of V_2. This can be proven using the same conditional expectation approach employed for $\widehat{V}_1$. Thus, define

$$\widehat{\text{var}}\{\widetilde{N}\} = \widehat{V}_1 + \widehat{V}_2 \tag{50}$$

as the asymptotically unbiased estimate of the sampling variance of $\widetilde{N}$.

In Section 3.4 we described how to estimate the variance of $1/\widehat{E}$ and the justification for treating $\widehat{E}$ and $\widetilde{N}$ as independent. Now

$$\widehat{N} = \widetilde{N} \Big/ \widehat{E} \tag{51}$$

and we can estimate the variance of $\widehat{N}$ as the variance of the product of independent random variables:

$$\widehat{\text{var}}\{\widehat{N}\} = \frac{1}{\widehat{E}^2}\widehat{\text{var}}\{\widetilde{N}\} + \widetilde{N}^2\widehat{\text{var}}\{1/\widehat{E}\} + \widehat{\text{var}}\{\widetilde{N}\}\widehat{\text{var}}\{1/\widehat{E}\}. \tag{52}$$

Wong (1996) has demonstrated (in the simpler case described in the next section) that it is better to estimate a confidence interval for N by applying a normal approximation to log abundance and then back-transforming the result. If we define $\widehat{CV}^2 = \widehat{\text{var}}\{\widehat{N}\}/\widehat{N}^2$, the estimated 95% confidence interval for N is

$$\left(\widehat{N}\exp\{-1.96\widehat{CV}\},\ \ \widehat{N}\exp\{1.96\widehat{CV}\}\right). \tag{53}$$

Estimation of N_4 for Trend

In Section 3.6 we note that an estimate of N_4 is needed for 2011 in order to include the 2011 abundance estimate in an updated trend estimate replicating past methods. Since our abundance estimation approach does not produce $\widehat{N}_4$, we must find an equivalent.

We take the approach of setting $\widehat{N}_4$ equal to the abundance estimate that we would have obtained if no corrections a_i for availability were made. This mimics the notion that N_4 is an abundance index that does not correct for P_4.

In this case, the results of Steinhorst and Samuel (1989) and Wong (1996) apply directly. If we re-define

$$\theta_i = 1/p_i$$

and interpret the remaining notation accordingly, then our estimate of N_4 is

$$\widehat{N}_4 = \frac{1}{\widehat{E}}\sum_1^g c_i\widehat{\theta}_i \tag{54}$$

where

$$\widehat{\theta}_i \ \ = \ \ 1 + \exp\{-\widehat{\mu}_i - \phi_i/2\}. \tag{55}$$

The variance and covariance estimators for $\widehat{\theta}_i$ are

$$\widehat{\text{var}}\{\widehat{\theta}_i\} \ \ = \ \ \exp\{-2\widehat{\mu}_i - 2\phi_i\}\left(\exp\{\phi_i\} - 1\right)$$

and

$$\widehat{\text{cov}}\{\widehat{\theta}_i, \widehat{\theta}_j\} \ \ = \ \ \exp\{-\widehat{\mu}_i - \widehat{\mu}_j - \widetilde{\phi}_{ij}\}\left(\exp\{\phi_{ij}\} - 1\right)$$

(Steinhorst and Samuel, 1989). Wong (1996) shows that the variance component estimates should remain as in (47) and (49) with the obvious reinterpretation of the notation. The results in (50), (51) and (52) also still pertain. Finally, we set $\widehat{N}_4 = \widehat{N}$ with variance as in (52).